Real-time Polymer Electrolyte Membrane Fuel Cell Parameter Estimation in Absence of Excitation

Andreu Cecilia[a,b,*], Maria Serra[c], Ramon Costa-Castelló[a]

[a] Universitat Politècnica de Catalunya, Diagonal 647, 08028, Barcelona, Spain
[b] Univ. Lyon, Université Claude Bernard Lyon 1, CNRS, LAGEPP UMR5007, Villeurbanne, F-69100, France
[c] Institut de Robòtica i Informàtica Industrial, CSIC-UPC, Llorens i Artigas 4-6, 08028 Barcelona, Spain

Abstract

Parameter estimation is crucial for polymer electrolyte membrane fuel cell monitoring and control. Nonetheless, most parameter estimation algorithms rely on a persistence of excitation condition, which is rarely satisfied and not convenient in fuel cell systems. For this reason, this work presents and compares three algorithms to estimate in real-time some critical PEMFC parameters in the voltage equation: the ohmic resistance, the charge transfer coefficient and the oxygen activity of a proton exchange fuel cell. The first algorithm is a standard gradient descent, while the other two are based on a set of pre-preprocessing dynamics. It is shown that, while the gradient descent requires the persistence of excitation condition, the addition of the pre-processing dynamics ensures reliable estimation under significantly weaker excitation assumptions. Moreover, it is shown that the pre-processing dynamics improves the transient behaviour and noise performance of the estimators. The results are validated through a set of numerical simulations and in an experimental prototype, where sensor noise and unmodelled disturbances are considered.

Keywords: Polymer electrolyte membrane fuel cell (PEMFC), Parameter estimation, Persistence of Excitation, Ohmic resistance

1. Introduction

Degradation issues limit the technical and economical viability of polymer electrolyte membrane fuel cells (PEMFCs) [1]. For example, in the context of vehicular applications, existing research shows that variable operating conditions including, but not restricted to, variable load, start-stop and idle speed, are the main reason for fuel cell degradation [2, 3]. Indeed, frequent load changes induce significant variations of multi-dimensional internal states, which have to be properly managed to guarantee adequate operation, performance and life-span of the system. This context has motivated the development of several algorithms to operate the PEMFC. Precisely, fault diagnosis algorithms have been developed to detect and ensure that the system is operating in a secure, safe and reliable manner [4]. Prognostics algorithms have been designed to estimate the State-of-Health of the system [5]. Observers have been proposed to monitor in real-time the unmeasured internal-states of the PEMFC [6] and multiple control algorithms have been proposed to adequately operate the PEMFC [7]. It should be mentioned that most of these algorithms are designed and implemented using a mathematical model of the PEMFC dynamics. This consideration is one of the reasons that have motivated the development of novel PEMFC mathematical models [8–10]. Furthermore, all the commented algorithms have to be implemented in real-time, which motivates the development of computational efficient models that can run in parallel to the PEMFC operation [11, 12].

In this line of research, a significant obstacle is that PEM-

*Corresponding author.
Email address: andreu.cecilia@upc.edu (Andreu Cecilia)

FCs dynamics are described by highly nonlinear and uncertain equations, where multiple parameters may be unknown and of time-varying nature. This lack of parameter knowledge stems from two reasons. First, the presence of certain electrochemical processes that are difficult to measure. Second, the approximations that are considered in order to reduce the computational complexity of the model. It should be remarked that the knowledge of these parameters is crucial for deploying model-based PEMFC algorithms. For this reason, there is a necessity of exploiting real-time parameter estimation algorithms to compute online the unknown model parameters from easily measurable data [13–18].

Real-time parameter estimation algorithms have been deeply studied in the past decades and have been used in a wide variety of systems. Commonly, these algorithms generate a consistent estimation by minimizing the observed error through a gradient descent algorithm [19], least-squares method [20], high-order sliding mode differentiators [21] or neural-network methods [22]. Nonetheless, the accuracy and robustness of these estimators is based on a **persistence of excitation** assumption [23]. That is, the inputs of the system have to "move" the system internal states such that the effect of the parameters can be noticed from the measured signals. Indeed, it is obvious that the measured signals need to contain enough information to derive the unknown parameters. What is not obvious is that this excitation condition needs to be satisfied persistently, that is, for all time. Therefore, if at any moment of the PEMFC operation the excitation condition is not satisfied, the real-time parameter estimation algorithm is immediately degraded, may provide unreliable estimations and may become numerically unstable. Moreover, to minimize degradation issues, PEMFCs systems usually require minimal input variations, thus, the excitation condition may not be satisfied in a persistent manner and may be undesirable for these systems. This is a critical limitation that prevents the practical application of such algorithms in PEMFCs and, to the authors' best knowledge, has been obviated in the PEMFC literature.

Multiple authors from the control community have proposed novel real-time parameter estimation algorithms that overcome this excitation limitation [23–28]. Precisely, the stringent **persistence of excitation** condition, that is rarely satisfied in PEMFC, is relaxed to a much less restrictive **interval excitation** condition that can be satisfied in PEMFC systems. The main objective of this work is to implement some of these algorithms in a PEMFC parameter estimation problem and to study its benefits in relation to more common options. To the best of the authors' knowledge, this is the first time that these algorithms are implemented in a PEMFC system. The main contributions of this work can be summarized as follows:

- Three algorithms to estimate in real-time the unknown parameters in the PEMFC voltage equation are proposed. The first one is a standard gradient descent. The other two are algorithms that can be implemented in the absence of persistence of excitation.
- The algorithms are compared through a set of numerical simulations, where sensor noise, unmodelled disturbances and the lack of persistence of excitation is considered.
- The reliability of the algorithms is compared in a PEMFC experimental prototype.

The remainder of this paper can be summarized as follows. Section 2 presents the PEMFC mathematical model and presents the main objectives of this work. Section 3 formulates these objectives as a parameter estimation problem. Section 4 presents the three algorithms that are implemented to solve the parameter estimation problem. Section 5 compares the algorithms in a set of numerical simulations. Section 6 validates and compares the algorithms in a real experimental prototype. Finally, some conclusions are drawn in Section 7.

2. Fuel cell model and objectives

Electrochemical models are used to predict PEMFC voltage by combining the theoretical maximum cell potential, E_r, with the major potential losses. That is, the ohmic losses, V_{ohm}, and the cathode activation polarization losses, $V_{act,c}$ [29]:

$$V = n_{cell}(E_r - V_{ohm} - V_{act,c}), \tag{1}$$

where n_{cell} is the number of cells in the fuel cell stack.

It should be mentioned that the voltage equation in (1) is not the most general one, but provides an adequate voltage prediction for a wide range of PEMFC operating conditions. Indeed, in general, the anode activation polarization losses are order of magnitudes lower than $V_{act,c}$. For this reason, the anode activation losses can be neglected. Moreover, due to degradation issues, it is usually undesirable to operate the PEMFC at high current densities where concentration losses become significant. For this reason, concentration losses have also been obviated.

The potential losses are related to the operating conditions of the PEMFC. Specifically, the ohmic losses are computed through the Ohm's law. That is,

$$V_{ohm} = R_{ohm} I,$$

where R_{ohm} is the ohmic resistance and I is the PEMFC current. The activation losses $V_{act,c}$ are computed through the following expression

$$V_{act,c} = \frac{RT}{2\alpha_c F} \ln\left(\frac{I}{A\ i_{o,c}}\right),$$

where α_c is the charge transfer coefficient, F is the Faraday's constant, R is the ideal gas constant, T is the fuel cell temperature and A is the cell active area. The factor $i_{o,c}$ depicts the exchange current density at the cathode layer, which is related to the PEMFC temperature, T, and physical properties and conditions of the catalyst layer

$$i_{o,c} = \gamma_c \sqrt{a_{O_2}} \exp\left[-\frac{E_{ca}}{RT}\left(1 - \frac{T}{293}\right)\right], \tag{2}$$

where γ_c is the exchange current density at reference conditions, a_{O_2} is the oxygen activity in the catalyst layer and E_{ca} is the activation energy of the reaction.

Although the electrochemical model of the fuel cell is relatively simple, the model contains a trio of parameters that cannot be directly measured and can vary depending on the PEMFC operating conditions. Indeed, the charge transfer coefficient, α_c, may vary according to the degradation level of the catalyst layer. Furthermore, the ohmic resistance, R_{ohm}, strongly depends on the water content of the membrane, which may vary depending on the temperature and humidity conditions in the inlet channels, the fuel cell membrane temperature and the amount of water generated due to the reduction reaction. Finally, the factor $\gamma_c \sqrt{a_{O_2}}$ depends on the oxygen concentration in the cathode catalyst layer, which varies according to the oxygen concentration in the inlet channels, the diffusion constants in the porous media and amount of oxygen consumed in the catalyst layer. The rest of parameters can be assumed to be known and fixed.

The main objective of this work is to develop an algorithm that can infer the value of the parameters, R_{ohm}, α_c and $\gamma_c \sqrt{a_{O_2}}$, in real-time. The capability of estimating these parameters in real-time has interesting practical implications. On the one hand, even if the parameters are unknown or change during the PEMFC operation, allows the real-time computation of the voltage equation in (1). On the other, as the value of each parameter is related to a particular operating conditions of the fuel cell, its estimation can be used to monitor and diagnose the system. For example, a low value in the ohmic resistance, R_{ohm}, may be related to a dry membrane operating condition.

Finally, it is convenient to design such algorithm based only on easy to measure signals as the current I, the stack voltage V and the fuel cell temperature T. This decision prevents the need of adding additional sensors or complex computing equipment in order to implement the algorithm.

3. Problem formulation

To ease the design of a real-time parameter estimation algorithm for the PEMFC, it is convenient to re-formulate the electrochemical model presented in Section 2 as a linear regression equation. Precisely, consider that a measured signal, $y \in \mathbb{R}$, and a vector of unknown parameters, $\boldsymbol{\theta} \in \mathbb{R}^q$, are related through a linear regression equation of the form

$$y = \boldsymbol{\phi}^\top \boldsymbol{\theta}, \tag{3}$$

where y and $\boldsymbol{\phi} \in \mathbb{R}^q$ are bounded measurable and known signals and $\boldsymbol{\theta} \in \mathbb{R}^q$ is a vector of constant unknown parameters. Usually, the factor $\boldsymbol{\phi}$ is denoted as the **regressor vector**.

To re-write the fuel cell model in Section 2 in the form (3) consider the following signal

$$y = \frac{V}{n_{cell}} - E_r. \tag{4}$$

Then, it can be shown that the regression equation in (3) is satisfied with

$$\begin{aligned} \boldsymbol{\phi}^\top &= \begin{bmatrix} -I & -\frac{RT}{2F}\left[\frac{E_{ca}}{RT}\left(1 - \frac{T}{293}\right) + \ln\left(\frac{I}{A}\right)\right] & \frac{RT}{2F} \end{bmatrix} \\ \boldsymbol{\theta}^\top &= \begin{bmatrix} \theta_1 & \theta_2 & \theta_3 \end{bmatrix} = \begin{bmatrix} R_{ohm} & \frac{1}{\alpha_c} & \frac{\ln(\gamma_c \sqrt{a_{O_2}})}{\alpha_c} \end{bmatrix}. \end{aligned} \tag{5}$$

It should be mentioned that the regressor vector, $\boldsymbol{\phi}$, can be computed using the PEMFC temperature, T, and the exchange current, I. Moreover, notice that the parameters $\boldsymbol{\theta}$ and the unknown PEMFC parameters are related through the following set of expressions

$$R_{ohm} = \theta_1, \quad \alpha_c = \frac{1}{\theta_2}, \quad \gamma_c \sqrt{a_{O_2}} = \exp\left(\frac{\theta_3}{\theta_2}\right). \tag{6}$$

That is, if the unknown parameters $\boldsymbol{\theta}$ are correctly estimated, the unknown PEMFC voltage parameters, R_{ohm}, α_c and $\gamma_c \sqrt{a_{O_2}}$, can be recovered through the expressions in (6). With this in mind, the main objective of this work is to design a real-time estimation algorithm that, based on the value of the measured signal, y, and the regressor vector, $\boldsymbol{\phi}$, generates an estimation of the unknown parameters, $\hat{\boldsymbol{\theta}}$, such that

$$\lim_{t\to\infty} |\boldsymbol{\theta} - \hat{\boldsymbol{\theta}}(t)| = 0. \tag{7}$$

4. Proposed parameter estimation algorithms

This section presents three different parameter estimation algorithms to solve the proposed parameter estimation problem. This section does not focus in any particular fuel cell model and presents the algorithms in a general manner. Thus, the presented algorithms are not restricted to the particular problem considered.

4.1. Algorithm 1: Classical gradient-descent

This subsection recalls the well-known gradient descent estimator. Although the material of this section is well-known, it has been included to make the document self-contained.

In its most basic form, a gradient-descent estimator of the unknown parameters, $\boldsymbol{\theta}$, of a linear regression of the form (3) is given by the following equation

$$\dot{\hat{\boldsymbol{\theta}}} = \boldsymbol{\Gamma}_{gd}\boldsymbol{\phi}(y - \boldsymbol{\phi}^\top\hat{\boldsymbol{\theta}}), \tag{8}$$

where $\boldsymbol{\Gamma}_{gd} = \boldsymbol{\Gamma}_{gd}^\top > 0$ is the adaptation gain of the estimator.

Before presenting the main convergence properties of the gradient-descent estimator in (8), the concept of **persistence of**

excitation has to be introduced.

Definition 4.1. *A bounded vector signal $\boldsymbol{\phi}(t) \in \mathbb{R}^q$ is said to be persistently excited if there exist some positive constant $T > 0$ such that*

$$\int_t^{t+T} \boldsymbol{\phi}(\tau)\boldsymbol{\phi}(\tau)^\top d\tau > 0, \quad \forall t \geq 0. \tag{9}$$

Roughly speaking, persistence of excitation establishes that for any time t the trajectory of the measured signal y in (3) from t to $t + T$ contains enough information to infer the unknown parameters $\boldsymbol{\theta}$. Notice that this property has to be satisfied in a persistent manner, that is, for all time instants t.

With this definition in mind, the main convergence properties of the gradient-descent estimator in (8) can be established [19, 20]. Indeed, assume that the regressor vector $\boldsymbol{\phi}$ of the linear regression (3) is persistently exciting as in Definition 4.1. Then, the gradient-descent equation in (8) satisfies the convergence property in (7).

It should be remarked that, in practice, it is very difficult to achieve the persistence of excitation condition in a PEMFC. Indeed, it is well-known that the identification of the ohmic resistance, R_{ohm}, requires high-frequency modulations of the PEMFC current, while the identification of the parameters in the activation polarization losses is reserved to low-frequencies [30–32]. Consequently, the persistence of excitation condition in Definition 4.1 requires a high-frequency and low-frequency modulation of the current, I, and a low-frequency modulation of the PEMFC temperature, T. This variation of the current and temperature will have an inevitable impact on the performance and degradation of the PEMFC. Notice that this modulation of current and temperature has to be maintained uninterruptedly, otherwise, once the variation is stopped, the algorithm may lose the convergence property (7) and the estimation $\hat{\boldsymbol{\theta}}$ may drift to an erroneous value. This fact, makes the classic gradient descent in (8) unreliable in practice.

It should be mentioned that some authors implement a recursive least-squares algorithm [13] instead of the classic gradient descent in (8), due to its better transient behaviour and noise performance. The only difference between the continuous time recursive least-squares and the gradient-descent is that the gain matrix $\boldsymbol{\Gamma}_{gd}$ is time-varying and computed through the following dynamics

$$\dot{\boldsymbol{\Gamma}}_{gd} = -\boldsymbol{\Gamma}_{gd}\boldsymbol{\phi}\boldsymbol{\phi}^\top\boldsymbol{\Gamma}_{gd}.$$

Nonetheless, the convergence of the estimation to the true value still requires the persistence of excitation condition [33, Section 4.4.2.2]. For this reason, the recursive least squares algorithm has been obviated in this work.

4.2. Algorithm 2: Gradient descent + pre-processing dynamics (GD+PD)

This subsection introduces the algorithm presented in [25]. In this algorithm, the signals y and $\boldsymbol{\phi}$ are pre-processed by a set of dynamics before introducing them to the gradient descent algorithm. It is proven in [25] that such processing improves the transient performance of the estimator and ensures the convergence of the estimation under less restrictive excitation assumptions.

Precisely, first, the signals y and $\boldsymbol{\phi}$ are processed through the following set of dynamics

$$\begin{aligned} \dot{\boldsymbol{\eta}} &= \alpha_1 \boldsymbol{\Omega}\boldsymbol{\phi}(y - \boldsymbol{\phi}^\top\boldsymbol{\eta}), \quad \boldsymbol{\eta}(0) = \begin{bmatrix} 0 & 0 & 0 \end{bmatrix}^\top, \\ \dot{\boldsymbol{\Omega}} &= -\alpha_1 \boldsymbol{\phi}\boldsymbol{\phi}^\top\boldsymbol{\Omega}, \quad \boldsymbol{\Omega}(0) = \mathbf{I}_3 \end{aligned} \tag{10}$$

where $\mathbf{I}_3$ is the identity matrix of order 3, $\alpha_1 > 0$ is a parameter to be tuned, $\boldsymbol{\eta} \in \mathbb{R}^3$ and $\boldsymbol{\Omega} \in \mathbb{R}^{3\times3}$ are the pre-processing dynamics internal variables. Intuitively, the equations in (10) serve as some kind of "memory dynamics" that store the parts of the measured signal trajectory that are exciting.

Second, the variables $\boldsymbol{\eta}$ and $\boldsymbol{\Omega}$ are used to compute a new signal, $\mathbf{y}_{pd}$, and a new regressor vector $\boldsymbol{\phi}_{pd}$

$$\begin{aligned}\mathbf{y}_{pd} &= \mathrm{adj}\{\mathbf{I}_3 - \boldsymbol{\Omega}\}\boldsymbol{\eta}\\ \boldsymbol{\phi}_{pd} &= \det\{\mathbf{I}_3 - \boldsymbol{\Omega}\},\end{aligned} \tag{11}$$

where $\det\{\cdot\}$ is the determinant and $\mathrm{adj}\{\cdot\}$ is the adjugate. The operations in (11) serve to diagonalize the matrix $\boldsymbol{\Omega}$. The authors in [24] proves that these operations significantly improve the transient performance of the parameter estimation algorithm.

Finally, the classic gradient descent in (8) is implemented over the new measured signal $\mathbf{y}_{pd}$ and the new regressor vector $\boldsymbol{\phi}_{pd}$. That is,

$$\dot{\hat{\boldsymbol{\theta}}} = \boldsymbol{\Gamma}_{A2}\boldsymbol{\phi}_{pd}(\mathbf{y}_{pd} - \boldsymbol{\phi}_{pd}^{\top}\hat{\boldsymbol{\theta}}), \tag{12}$$

where $\boldsymbol{\Gamma}_{A2}$ is the adaptation gain of the estimator.

Before presenting the main convergence properties of the estimator in (12), it is important to introduce the notion of **interval excitation**.

Definition 4.2. *A bounded signal $\boldsymbol{\phi}(t) \in \mathbb{R}^q$ is said to be intervally excited if there exists a constant $t_c > 0$ such that*

$$\int_0^{t_c} \boldsymbol{\phi}(\tau)\boldsymbol{\phi}(\tau)^{\top} d\tau > 0.$$

It should be remarked that the interval excitation condition in Definition 4.2 is significantly less restrictive than the persistence of excitation condition in Definition 4.1. Indeed, persistence of excitation is a condition that has to be satisfied at all time instants t. Thus, persistent changes in the current and temperature have to be imposed on the PEMFC at all times, otherwise, the estimation $\hat{\boldsymbol{\theta}}$ of the gradient descent (8) may diverge. Alternatively, interval excitation only needs to be satisfied during a finite time t_c, which is a much more feasible assumption in PEMFC systems.

With this definition in mind, the main convergence properties of the estimator can be summarized as follows [25]. If the regressor vector $\boldsymbol{\phi}$ satisfies the interval excitation condition in Definition 4.2, then the GD+PD dynamics in (12) satisfy the convergence property in (7).

4.3. Algorithm 3: Gradient descent + pre-processing dynamics with forgetting factor (GD+PD+FF)

A limitation of the pre-processing dynamics in (10) is that the $\boldsymbol{\Omega}$ matrix can become arbitrarily small, which critically slows down the parameter estimation [33, Section 4.4.2.2]. To overcome this limitation, a new set of pre-processing dynamics where proposed in [28]. Specifically, similar to the algorithm in Subsection 4.2, the signals y and $\boldsymbol{\phi}$ are pre-processed through the following set of dynamics:

$$\begin{aligned}\dot{\boldsymbol{\eta}} &= \alpha_2\boldsymbol{\Omega}\boldsymbol{\phi}(y - \boldsymbol{\phi}^{\top}\boldsymbol{\eta}), & \boldsymbol{\eta} &= \begin{bmatrix}0 & 0 & 0\end{bmatrix}\\ \dot{\boldsymbol{\Omega}} &= -\alpha_2\boldsymbol{\Omega}\boldsymbol{\phi}\boldsymbol{\phi}^{\top}\boldsymbol{\Omega} + \beta(1 - |\boldsymbol{\Omega}|)\boldsymbol{\Omega}, & \boldsymbol{\Omega}(0) &= \boldsymbol{I}_3\\ \dot{z} &= -\beta(1 - |\boldsymbol{\Omega}|)z, & z(0) &= 1,\end{aligned} \tag{13}$$

where $\alpha_2 > 0$ and $\beta > 0$ are design parameters, $|\cdot|$ is the induced norm of the matrix and $\boldsymbol{\eta}, \boldsymbol{\Omega}, z$ are the pre-processing dynamics internal variables. Again, intuitively, the dynamics in (13) store the parts of the measured signal trajectory that are exciting. Nonetheless, different from the pre-processing dynamics in (10), the ones in (13) include a forgetting factor in the $\boldsymbol{\Omega}$ to slow down the convergence of the matrix $\boldsymbol{\Omega}$ to small values.

Then, the variables $\boldsymbol{\eta}, \boldsymbol{\Omega}$ and z are used to compute a new measured signal $\mathbf{y}_{pd}$ and regressor vector $\boldsymbol{\phi}_{pd}$ as follows

$$\begin{aligned}\mathbf{y}_{pd} &= \mathrm{adj}\{\mathbf{I}_3 - z\boldsymbol{\Omega}\}\boldsymbol{\eta}\\ \boldsymbol{\phi}_{pd} &= \det\{\mathbf{I}_3 - z\boldsymbol{\Omega}\}.\end{aligned} \tag{14}$$

Finally, the standard gradient-descent in (8) is applied over the signal $\mathbf{y}_{pd}$ and $\boldsymbol{\phi}_{pd}$

$$\dot{\hat{\boldsymbol{\theta}}} = \boldsymbol{\Gamma}_{A3}\boldsymbol{\phi}_{pd}(\mathbf{y}_{pd} - \boldsymbol{\phi}_{pd}^{\top}\hat{\boldsymbol{\theta}}), \tag{15}$$

where $\boldsymbol{\Gamma}_{A3}$ is the adaptation gain of the estimator.

The main convergence properties of the estimator can be summarized as follows [28]. If the regressor vector $\boldsymbol{\phi}$ satisfies the interval excitation condition in Definition 4.2, then the GD+PD+FF dynamics in (15) satisfies the convergence property in (7). Similar to the GD+PD in (12), the estimator in (15) ensures reliable parameter estimation under the less restrictive assumption of interval excitation.

5. Numerical Simulations

In this section, the performance of the 3 estimators is compared in 3 different case scenarios. In the first scenario case A, it is assumed an ideal situation where the voltage sensor is free of noise and there are no unmodelled disturbances. In the Case B, it is assumed that the measured stack voltage is corrupted by white noise. Finally, in the Case C, it will be assumed that the linear regression equation (3) is affected by an unknown additive time-varying disturbance.

In all the simulations, the model presented and experimentally validated in [34] will be used as ground truth. That is, the model in [34] will be excited by some particular current profiles to generate the signals y and $\boldsymbol{\phi}$ that are used in the estimators to infer the value of the unknown parameters. Moreover, in all the simulations, a particular current profile, I, is used such that the regressor vector $\boldsymbol{\phi}$ is not persistently excited as in Definition 4.1 but is intervally excited as in Definition 4.2. As commented in Subsection 4.1 this is a common scenario in PEMFC systems.

The algorithms have been implemented with the parameters presented in Table 1. This parameters have been tuned to have an adequate trade-off between convergence rate and noise sensitivity.

5.1. Case A: Ideal scenario

The first case scenario considers the ideal situation where the voltage sensor is free of any noise and there are no unmodelled dynamics in the PEMFC model. The result of the simulation is presented in Figure 1.

Table 1: Estimation algorithms design parameters during simulations.

Parameter	Value
Algorithm 1	
$\boldsymbol{\Gamma}_{gd}$	$10 \cdot \boldsymbol{I}_3$
Algorithm 2	
α_1	1
$\boldsymbol{\Gamma}_{A2}$	$10 \cdot \boldsymbol{I}_3$
Algorithm 2	
α_2	2
β	2
$\boldsymbol{\Gamma}_{A2}$	$10 \cdot \boldsymbol{I}_3$

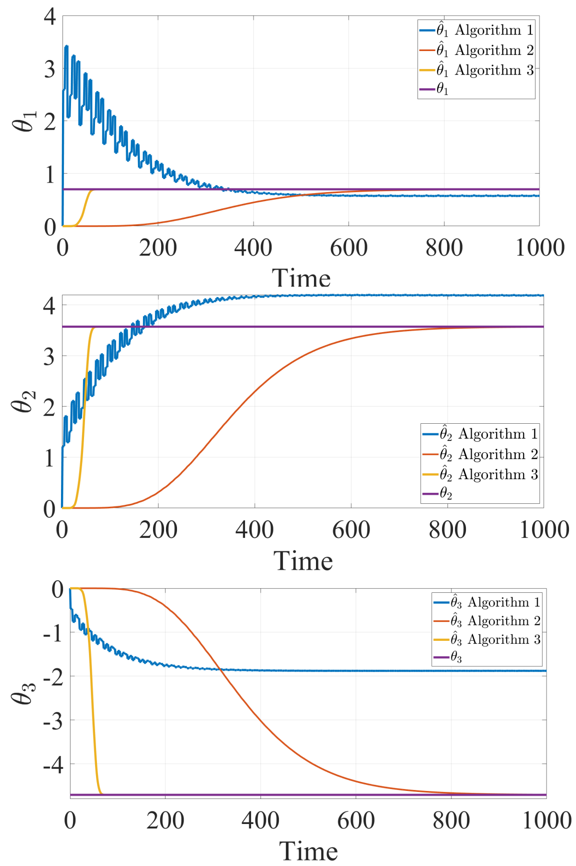

Figure 1: Simulation result in the ideal scenario. The purple line depicts the true value of the parameters. The rest of the lines are the estimation evolution of the presented algorithms.

This simulation exemplifies the effect of the lack of persistence of excitation (see Definition 4.1) on the quality of the estimation of the classic gradient descent (8). Indeed, even in the absence of noise and disturbances, the classic gradient descent (Algorithm 1) cannot converge to the true value of the parameters, due to the absence of excitation.

Alternatively, the benefits of the pre-processing dynamics of Algorithm 2 in (12) and Algorithm 3 in (15) can be noticed in Figure 1. First, the lack of persistence of excitation problem is solved and the parameter estimation converges to the true value. Second, the algorithms present better transient behaviour with respect to the classic gradient descent. Indeed, it can be observed that the gradient descent present significant oscillations, while Algorithm 2 and Algorithm 3 present a better monotonic convergence.

Finally, it can be observed that the Algorithm 3 presents significantly faster convergence rate than the other two algorithms. Precisely, while Algorithm 2 requires around 700 seconds to converge, Algorithm 3 converges in around 100 seconds.

5.2. Case B: Presence of sensor noise

The second case scenario compares the performance of the algorithms when the voltage sensor is affected by additive white noise of variance 0.1. It should be stated that this noise variance is significantly larger than the one expected in experimental set-ups. The result of the simulation is presented in Figure 2. Naturally, in this case scenario, the estimation does not converge to a constant value but converges to an oscillatory trajectory that is induced by the noise.

It can be seen that the classic gradient descent (Algorithm 1) (8) presents the worst performance of the three in two senses. First, for the same reasons discussed in Subsection 5.1, the lack of persistence of excitation makes the estimation of the gradient descent converge to a significantly biased value. Second, the gradient descent is very sensitive to sensor noise. That is, the accuracy of the estimation is significantly affected by the presence of noise. Indeed, Figure 1 shows that the gradient descent algorithm achieves an estimation of the parameter θ_1

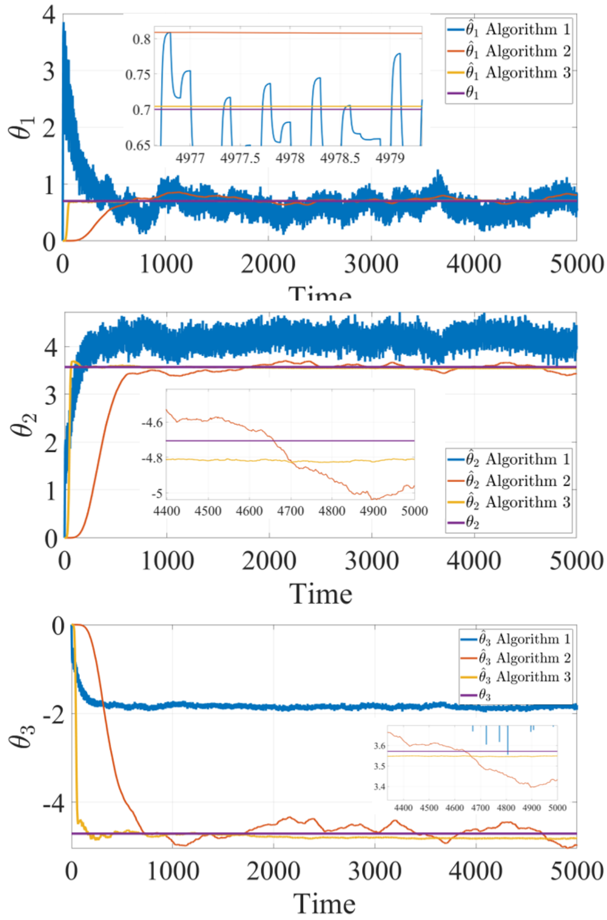

Figure 2: Simulation result in the presence of sensor noise. The purple line depicts the true value of the parameters. The rest of the lines are the estimation evolution of the presented algorithms.

with a relative error[1] of 18.1% in the absence of sensor noise. Meanwhile, Figure 2 shows that the same estimation converges to a relative error of 31.2% in the presence of sensor noise.

In relation to Algorithm 2 and Algorithm 3, it is noticeable that the estimations converges to an oscillatory trajectory of low frequency in relation to the classic gradient descent estimation. This behaviour appears due to the pre-processing dynamics, which have a low-pass filter property between the measured signal y and the generated signals $\mathbf{y}_{pd}$. Moreover, Algorithm 3 presents better estimation accuracy than Algorithm 2. Precisely, for the parameter θ_3, Algorithm 2 converges to a relative error of

[1]The relative error between a value x and its estimation $\hat{x}$ is computed as $\frac{|x-\hat{x}|}{|x|} \cdot 100$.

5.4% while Algorithm 3 converges to a relative error of 2.122%. Algorithm 3 also presents lower relative error in the estimation of the parameters $\hat{\theta}_1$ and $\hat{\theta}_3$.

5.3. Case C: Presence of additive disturbances

The last case scenario considers the situation where the regressor vector $\boldsymbol{\phi}$ is not perfectly modelled. That is, the equation in (3) does not model exactly the PEMFC voltage equation. Precisely, the estimation algorithm used as a regressor vector is disturbed as follows

$$\boldsymbol{\phi}^\top =$$
$$\left[-I + d \qquad -\frac{RT}{2F}\left[\frac{E_{ca}}{RT}\left(1 - \frac{T}{293}\right) + \ln\left(\frac{I}{A}\right)\right] + d \qquad \frac{RT}{2F} + d \right],$$

where d is a disturbance signal generated as a sinusoidal of the form $d = 0.1sin(0.1t)$. The results of the simulations are depicted in Figure 3.

For the same reasons discussed in Subsection 5.1 and Subsection 5.2 the classic gradient descent (Algorithm 1) converges to the largest relative error of the three.

Naturally, the presence of unmodelled elements prevents the convergence of the Algorithm 2 and Algorithm 3 to the true value. Nonetheless, the estimation of these algorithms converge to a relative error that is significantly lower than the one of the classic gradient descent. For example, for the third parameter, θ_3 the classic gradient descent converges to a relative error of 55.3%, the Algorithm 2 converges to a relative error of 5.5319% and the Algorithm 3 converges to a relative error of 7.8%. It is noticeable that in this case scenario, Algorithm 2 presents a slightly better accuracy than the Algorithm 3. This result validates the robustness of Algorithm 2 and Algorithm 3 with respect to unmodelled disturbances.

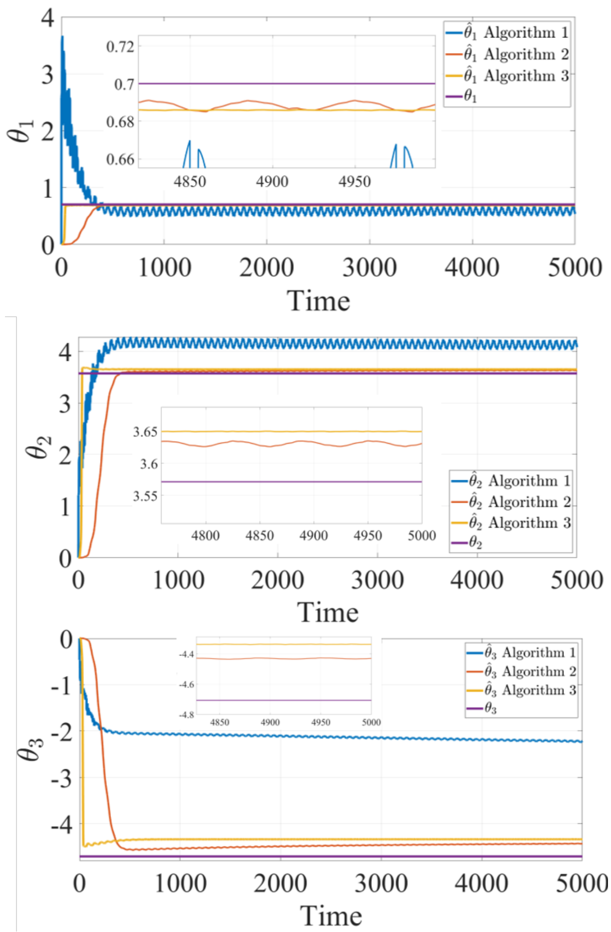

Figure 3: Simulation result in the presence of additive disturbances in the regressor vector. The purple line depicts the true value of the parameters. The rest of the lines are the estimation evolution of the presented algorithms.

6. Experimental Validation

6.1. Experimental Set-up

In this section, the presented algorithms will be compared in an experimental prototype. The experimental set-up incorporates a PEMFC model H-100 with an open-cathode architecture. In the cathode side, the stack includes a controlled fan that delivers ambient air. The controller of the fan is implemented through a NI-9505 PWM module of National Instruments. Moreover, a sensor model EE75 of E+E Elektronik is included in the cathode to measure the air velocity. In the anode side, pure hydrogen is delivered through a compressed cylinder. The set-up does not include any flow controller. Consequently, the PEMFC operates in purged dead-end mode [29] with a pressure regulator that maintains the anode inlet at 0.4 *bar*.

Due to its open-cathode architecture, the PEMFC is sensitive to the ambient temperature, humidity and gas composition. For this reason, the PEMFC is enclosed inside an environmental chamber that regulates humidity, oxygen concentration, and temperature.

The cell temperature is measured through a type K thermocouple. The temperature of the stack, T, is assumed to be the average of all cell temperatures.

The current can be modified through a programmable load that emulates some external energy demand. Finally, an isolation amplifier AD215 from Analog Devices is used to measure the stack voltage, v_{fc} and a Hall effect sensor model LTS 6 NP is implemented to measure the current.

A scheme of the set-up and a photography can be found in Fig. 4.

The signal y in (4) and the regressor vector, $\boldsymbol{\phi}$, require a set of parameters that have been tuned to the considered PEMFC model H-100. These parameters have been tuned following a particle swarm optimization approach similar to the one used in [14]. This set of parameters is presented in Table 2.

Table 2: H-100 model parameters during the experiment

Parameter	Description	Value
E_r	Theoretical cell potential	18.3816 V
n_{cell}	Number of cells	24
R	Ideal Gas constant	8.314 $J/(K\ mol)$
F	Faraday's constant	96485 C/mol
E_{ca}	Activation energy ORR	70000 J/mol
A	Area cathode catalyst layer	0.01 m^2

6.2. Methodology

A specific current profile is introduced in the PEMFC stack to generate a voltage, V, and temperature, T, profile. This signal values are depicted in Figure 5. The current profile has been designed to generate sufficient excitation in order to estimate the parameters.

The experimental profiles in Figure 5 and the parameter values in Table 2 are used to generate the signals y and $\boldsymbol{\phi}$ that are introduced in the presented algorithms to estimate the unknown parameters, $\boldsymbol{\theta}$.

It should be mentioned that the parameters $\boldsymbol{\theta}$ cannot be directly measured. Therefore, different from the numerical simulation analysis in Section 5, the estimation of the algorithms cannot be compared with any ground truth. Consequently, in order to validate the algorithms and compare its performance, a specific methodology has to be developed.

As it will be shown in the next subsection, each algorithm estimation converges to a different set of values at the end of the experiment. These values can be used to compare the performance of the algorithms. Precisely, once the algorithm has converged to a value, $\hat{\boldsymbol{\theta}}^*$, this value can be used to generate an estimation of the voltage signal as follows

$$\hat{V} = n_{cell}\ (E_r + \boldsymbol{\phi}^\top \hat{\boldsymbol{\theta}}^*)$$

where the regressor vector $\boldsymbol{\phi}$ is computed with the data in Figure 5 and the parameters in Table 2. Then, the accuracy of the estimated parameter, $\hat{\boldsymbol{\theta}}^*$, can be computed through the mean squared error between the estimated voltage, $\hat{V}$, and the measured voltage, V. That is,

$$MSE(\hat{\boldsymbol{\theta}}^*) = \frac{1}{n} \sum_{i=1}^{n} (V(i) - \hat{V}(i)), \tag{16}$$

where the sampling time to compute the mean squared error has been fixed at 2 seconds. The algorithm with the lower mean squared error computed through (16) can be concluded to be the most accurate.

Finally, it should be stated that the presented algorithms are implemented with the parameters in Table 3. The value of these parameters are significantly lower than the ones during

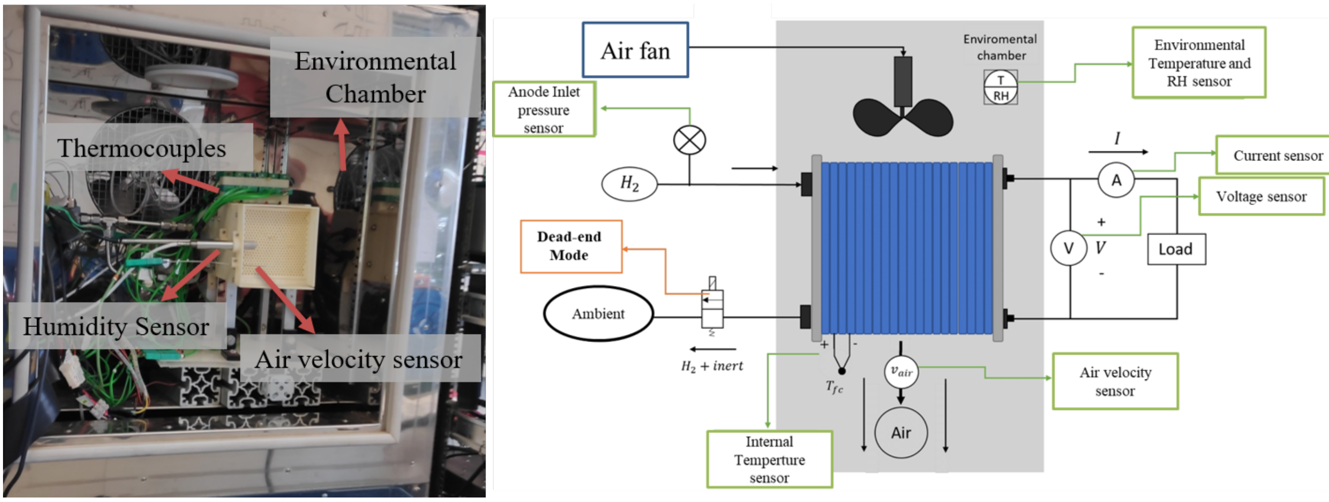

Figure 4: (a) Environmental chamber and H-100 PEMFC. (b) H-100 experimental set-up scheme.

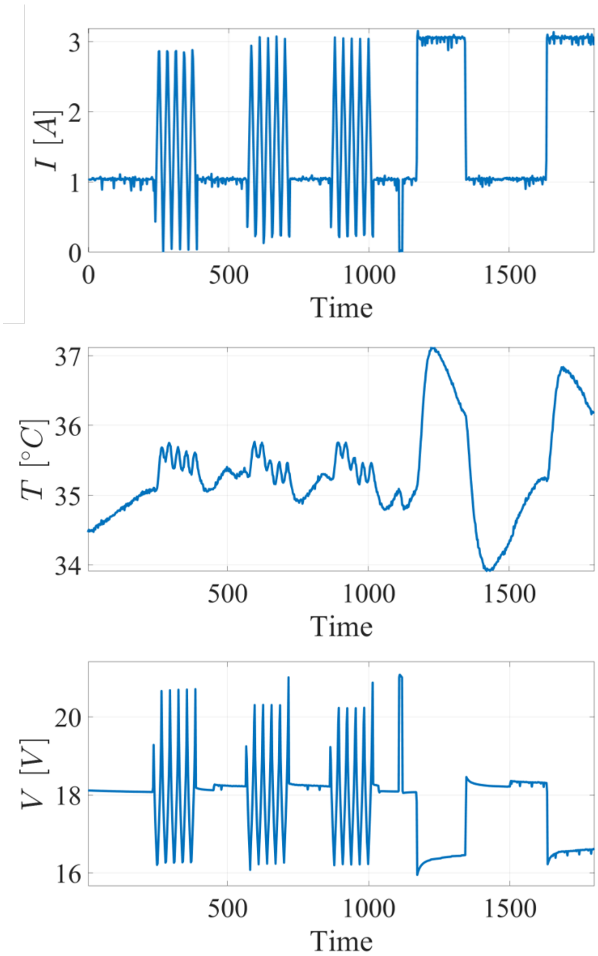

Figure 5: Sensor data of the PEMFC experiment.

the simulations (see Table 1). This reduction on the parameters slows down the convergence rate of the estimators, but, eases the practical implementation of the algorithms to the considered system with a sampling time of 2 seconds.

Table 3: Estimation algorithms design parameters during the experiment

Parameter	Value
Algorithm 1	
$\mathbf{\Gamma}_{gd}$	$0.1 \cdot \boldsymbol{I}_3$
Algorithm 2	
α_1	0.1
$\mathbf{\Gamma}_{A2}$	$5 \cdot \boldsymbol{I}_3$
Algorithm 2	
α_2	0.1
β	0.1
$\mathbf{\Gamma}_{A2}$	$5 \cdot \boldsymbol{I}_3$

6.3. Results and Discussion

The experimental data has been introduced in the Algorithm 1 in (8), the Algorithm 2 in (12) and the Algorithm 3 in (15). The generated estimation is depicted in Figure 6. Similar to the Numerical Simulations in Section 5, each algorithm presents a significantly different transient trajectory. Precisely, it can be seen that the classic gradient descent presents oscillatory behaviour, while the Algorithm 2 and Algorithm 3 presents a much “smoother" trajectory.

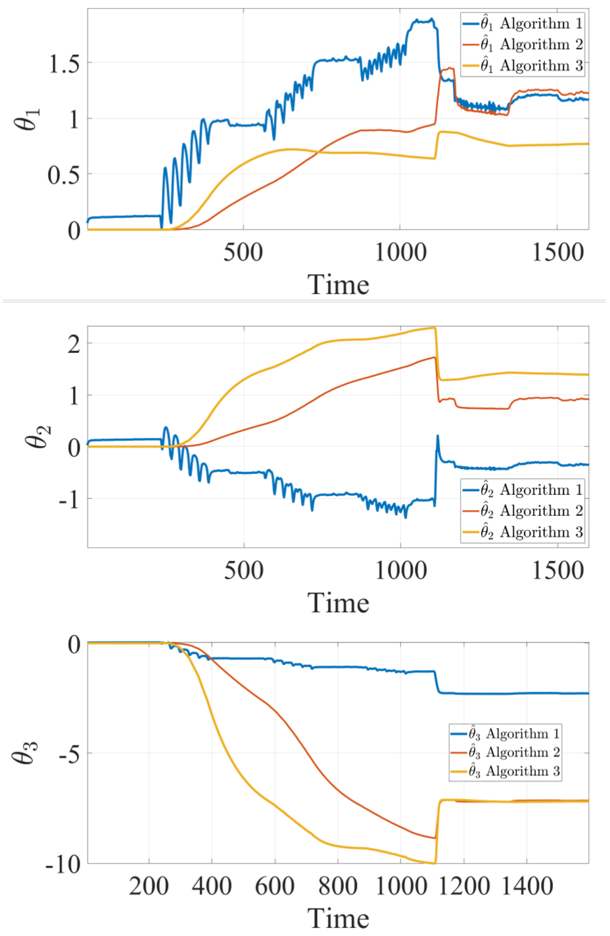

Figure 6: Unknown parameter estimation of the presented algorithms using experimental data.

Furthermore, it is noticeable that each algorithm has converged to a significantly different set of parameters. This result shows why selecting the adequate algorithm has a significant impact on the real-time parameter estimation problem. In order to compare the accuracy of each parameter estimation, the mean squared error (16) is computed in each algorithm. Precisely, the classic gradient descent presented a mean squared error of 0.1123, the Algorithm 2 presented a mean squared error of 0.1118 and the Algorithm 3 presented a mean squared error of 0.0295. This validates that the Algorithm 3 estimation has converged to a more accurate set of parameters in the experimental set-up.

7. Conclusions

This work has presented three algorithms to estimate in real-time parameters of the PEMFC voltage equation. The first algorithm is the classic gradient descent, while the other two are estimators that are based on a set of pre-processing dynamics. The main advantage of these pre-processing dynamics is that reliable estimation can be obtained under an interval of excitation condition, while the classic gradient descent (or recursive least squares) requires a more stringent persistence of excitation condition, that is rarely satisfied in PEMFCs. To the authors' best knowledge, this is the first time that a real-time parameter estimation algorithm that does not rely on the persistence of excitation condition has been proposed for a PEMFC system.

The benefits of Algorithm 2 and Algorithm 3 in front of the classic gradient descent have been validated through numerical simulations and in an experimental prototype. These benefits can be summarized as follows:

- Reliable estimation can be obtained in the absence of persistence of excitation.

- The transient behaviour of the estimation is improved.

Precisely, while the classic gradient descent presents oscillatory behaviour, Algorithm 2 and Algorithm 3 presents a much smoother convergence.

- The pre-processing dynamics acts as a low-pass filter, which reduces the effect of the sensor noise on the estimation.
- Adding disturbances to the regressor does not destabilize the pre-processing dynamics and the estimation error induced by these disturbances is reduced.

Finally, the numerical simulations and the experiment have been used to compare the performance between Algorithm 2 and Algorithm 3. From the numerical simulations, it can be concluded that Algorithm 3 presents much faster convergence rate than Algorithm 2. Moreover, Algorithm 3 is less sensitive to sensor noise. Nonetheless, in the presence of additive disturbances in the regressor vector, Algorithm 2 presented a slightly lower estimation error. The benefits of Algorithm 3 over Algorithm 2 have been further validated in the experimental prototype, where it has been shown that the parameters estimated through Algorithm 3 presented significantly better voltage prediction capabilities.

It should be remarked that these algorithms are not limited to the considered set of parameters, and can also be implemented to estimate other PEMFCs parameters. Indeed, it is expected that these algorithms can be utilized to estimate parameters related to the liquid water dynamics [16], where expecting a persistence of excitation condition is unfeasible.

Declaration of competing interest

The authors declare that they have no known competing financial interests or personal relationships that could have appeared to influence the work reported in this paper.

Acknowledgements

This work has been supported by the Spanish Ministry of Universities funded by the European Union - NextGenerationEU (2022UPC-MSC-93823).

This work is part of the Project MAFALDA (PID2021-126001OB-C31) funded by MCIN/ AEI /10.13039/501100011033 and by "ERDF A way of making Europe"

This work is part of the project MASHED (TED2021-129927B-I00), funded by MCIN/ AEI/10.13039/501100011033 and by the European Union Next GenerationEU/PRTR.

This research has been developed within the CSIC Interdisciplinary Thematic Platform (PTI+) Transición Energética Sostenible+ (PTI-TRANSENER+) as part of the CSIC program for the Spanish Recovery, Transformation and Resilience Plan funded by the Recovery and Resilience Facility of the European Union, established by the Regulation (EU) 2020/2094.

References

[1] S. Jomori, N. Nonoyama, T. Yoshida, Analysis and modeling of pemfc degradation: Effect on oxygen transport, Journal of Power Sources 215 (2012) 18–27. doi:https://doi.org/10.1016/j.jpowsour.2012.04.069.

[2] P. Pei, H. Chen, Main factors affecting the lifetime of proton exchange membrane fuel cells in vehicle applications: A review, Applied Energy 125 (2014) 60–75. doi:https://doi.org/10.1016/j.apenergy.2014.03.048.

[3] P. Pei, Q. Chang, T. Tang, A quick evaluating method for automotive fuel cell lifetime, International Journal of Hydrogen Energy 33 (14) (2008) 3829–3836, tMS07: Symposium on Materials in Clean Power Systems. doi:https://doi.org/10.1016/j.ijhydene.2008.04.048.

[4] A. Benmouna, M. Becherif, D. Depernet, F. Gustin, H. Ramadan, S. Fukuhara, Fault diagnosis methods for proton exchange membrane fuel cell system, International Journal of Hydrogen Energy 42 (2) (2017) 1534–1543. doi:https://doi.org/10.1016/j.ijhydene.2016.07.181. URL https://www.sciencedirect.com/science/article/pii/S0360319916307364

[5] M. Jouin, R. Gouriveau, D. Hissel, M.-C. Péra, N. Zerhouni, Prognostics and health management of pemfc – state of the art and remaining

challenges, International Journal of Hydrogen Energy 38 (35) (2013) 15307–15317. doi:https://doi.org/10.1016/j.ijhydene.2013.09.051.

[6] H. Yuan, H. Dai, X. Wei, P. Ming, Model-based observers for internal states estimation and control of proton exchange membrane fuel cell system: A review, Journal of Power Sources 468 (2020) 228376. doi:https://doi.org/10.1016/j.jpowsour.2020.228376.

[7] W. Daud, R. Rosli, E. Majlan, S. Hamid, R. Mohamed, T. Husaini, Pem fuel cell system control: A review, Renewable Energy 113 (2017) 620–638. doi:https://doi.org/10.1016/j.renene.2017.06.027.

[8] T. Jahnke, G. Futter, A. Latz, T. Malkow, G. Papakonstantinou, G. Tsotridis, P. Schott, M. Gérard, M. Quinaud, M. Quiroga, A. Franco, K. Malek, F. Calle-Vallejo, R. Ferreira de Morais, T. Kerber, P. Sautet, D. Loffreda, S. Strahl, M. Serra, P. Polverino, C. Pianese, M. Mayur, W. Bessler, C. Kompis, Performance and degradation of proton exchange membrane fuel cells: State of the art in modeling from atomistic to system scale, Journal of Power Sources 304 (2016) 207–233. doi:https://doi.org/10.1016/j.jpowsour.2015.11.041.

[9] C. Siegel, Review of computational heat and mass transfer modeling in polymer-electrolyte-membrane (pem) fuel cells, Energy 33 (9) (2008) 1331–1352. doi:https://doi.org/10.1016/j.energy.2008.04.015.

[10] A. Shah, K. Luo, T. Ralph, F. Walsh, Recent trends and developments in polymer electrolyte membrane fuel cell modelling, Electrochimica Acta 56 (11) (2011) 3731–3757. doi:https://doi.org/10.1016/j.electacta.2010.10.046.

[11] A. Goshtasbi, B. L. Pence, T. Ersal, Computationally efficient pseudo-2d non-isothermal modeling of polymer electrolyte membrane fuel cells with two-phase phenomena, Journal of The Electrochemical Society 163 (13) (2016) F1412. doi:10.1149/2.0871613jes.

[12] J. T. Pukrushpan, H. Peng, A. G. Stefanopoulou, Control-Oriented Modeling and Analysis for Automotive Fuel Cell Systems , Journal of Dynamic Systems, Measurement, and Control 126 (1) (2004) 14–25. doi:10.1115/1.1648308.

[13] K. Ettihir, L. Boulon, M. Becherif, K. Agbossou, H. Ramadan, Online identification of semi-empirical model parameters for pemfcs, International Journal of Hydrogen Energy 39 (36) (2014) 21165–21176. doi:https://doi.org/10.1016/j.ijhydene.2014.10.045.

[14] Y. Xing, J. Na, M. Chen, R. Costa-Castelló, V. Roda, Adaptive nonlinear parameter estimation for a proton exchange membrane fuel cell, IEEE Transactions on Power Electronics 37 (8) (2022) 9012–9023. doi:10.1109/TPEL.2022.3155573.

[15] Y. Xing, J. Na, R. Costa-Castelló, Real-time adaptive parameter estimation for a polymer electrolyte membrane fuel cell, IEEE Transactions on Industrial Informatics 15 (11) (2019) 6048–6057. doi:10.1109/TII.2019.2915569.

[16] A. Cecilia, M. Serra, R. Costa-Castelló, Nonlinear adaptive observation of the liquid water saturation in polymer electrolyte membrane fuel cells, Journal of Power Sources 492 (2021) 229641. doi:https://doi.org/10.1016/j.jpowsour.2021.229641.

[17] Y. Xing, L. Bernadet, M. Torrell, A. Tarancón, R. Costa-Castelló, J. Na, Offline and online parameter estimation of nonlinear systems: Application to a solid oxide fuel cell system, ISA Transactions (2022). doi:https://doi.org/10.1016/j.isatra.2022.07.025.

[18] A. Cecilia, R. Costa-Castelló, High gain observer with dynamic deadzone to estimate liquid water saturation in pem fuel cells, Revista Iberoamericana de Automática e Informática industrial 17 (2) (2020) 169–180.

[19] P. A. Ioannou, J. Sun, Robust adaptive control, Courier Corporation, 2012.

[20] S. Sastry, M. Bodson, J. F. Bartram, Adaptive control: stability, convergence, and robustness (1990).

[21] P. Fornaro, T. Puleston, P. Puleston, M. Serra-Prat, R. Costa-Castelló, P. Battaiotto, Redox flow battery time-varying parameter estimation based on high-order sliding mode differentiators, International Journal of Energy Research 46 (12) (2022) 16576–16592. doi:https://doi.org/10.1002/er.8319.

[22] R. Hecht-Nielsen, Kolmogorov's mapping neural network existence theorem, in: Proceedings of the international conference on Neural Networks, Vol. 3, IEEE Press New York, NY, USA, 1987, pp. 11–14.

[23] R. Ortega, V. Nikiforov, D. Gerasimov, On modified parameter estimators for identification and adaptive control. a unified framework and some new schemes, Annual Reviews in Control 50 (2020) 278–293. doi:https://doi.org/10.1016/j.arcontrol.2020.06.002.

[24] S. Aranovskiy, A. Bobtsov, R. Ortega, A. Pyrkin, Performance enhancement of parameter estimators via dynamic regressor extension and mixing, IEEE Transactions on Automatic Control 62 (7) (2017) 3546–3550. doi:10.1109/TAC.2016.2614889.

[25] L. Wang, R. Ortega, A. Bobtsov, J. G. Romero, B. Yi, Identifiability implies robust, globally exponentially convergent on-line parameter estimation: Application to model reference adaptive control, arXiv preprint arXiv:2108.08436 (2021).

[26] R. Marino, P. Tomei, On exponentially convergent parameter estimation with lack of persistency of excitation, Systems & Control Letters 159 (2022) 105080. doi:https://doi.org/10.1016/j.sysconle.2021.105080.

[27] G. Chowdhary, T. Yucelen, M. Mühlegg, E. N. Johnson, Concurrent learning adaptive control of linear systems with exponentially convergent

bounds, International Journal of Adaptive Control and Signal Processing 27 (4) (2013) 280–301. doi:https://doi.org/10.1002/acs.2297.

[28] R. Ortega, J. G. Romero, S. Aranovskiy, A new least squares parameter estimator for nonlinear regression equations with relaxed excitation conditions and forgetting factor, arXiv preprint arXiv:2205.00099 (2022).

[29] F. Barbir, PEM fuel cells: theory and practice, Academic press, 2012.

[30] A. Husar, S. Strahl, J. Riera, Experimental characterization methodology for the identification of voltage losses of pemfc: Applied to an open cathode stack, International Journal of Hydrogen Energy 37 (8) (2012) 7309–7315, iII Iberian Symposium on Hydrogen, Fuel Cells and Advanced Batteries, HYCELTEC-2011. doi:https://doi.org/10.1016/j.ijhydene.2011.11.130.

[31] M. Baghalha, J. Stumper, M. Eikerling, Model-based deconvolution of potential losses in a pem fuel cell, ECS Transactions 28 (23) (2010) 159. doi:10.1149/1.3502347.

[32] J. Wu, X. Z. Yuan, H. Wang, M. Blanco, J. J. Martin, J. Zhang, Diagnostic tools in pem fuel cell research: Part i electrochemical techniques, International Journal of Hydrogen Energy 33 (6) (2008) 1735–1746. doi:https://doi.org/10.1016/j.ijhydene.2008.01.013.

[33] J. A. Farrell, M. M. Polycarpou, Adaptive approximation based control: unifying neural, fuzzy and traditional adaptive approximation approaches, John Wiley & Sons, 2006.

[34] S. Strahl, A. Husar, P. Puleston, J. Riera, Performance improvement by temperature control of an open-cathode pem fuel cell system, Fuel Cells 14 (3) (2014) 466–478. doi:https://doi.org/10.1002/fuce.201300211.